Molecular Crystals and Liquid Crystals

ISSN: 1542-1406 (Print) 1563-5287 (Online) Journal homepage: http://www.tandfonline.com/loi/gmcl20

Mn^{II} Complexes with a Novel Triacid as Ligand: Synthesis and Characterization

Dehai Zhao, Zhenjun Si, Tao Shi, Qian Duan & Linfang Shi

To cite this article: Dehai Zhao, Zhenjun Si, Tao Shi, Qian Duan & Linfang Shi (2014) Mn^{II} Complexes with a Novel Triacid as Ligand: Synthesis and Characterization, Molecular Crystals and Liquid Crystals, 605:1, 179-186, DOI: 10.1080/15421406.2014.885360

To link to this article: http://dx.doi.org/10.1080/15421406.2014.885360

Molecular Crystals and Liquid Crystals, Vol. 605: pp. 179–186, 2014

ISSN: 1542-1406 print/1563-5287 online
DOI: 10.1080/15421406.2014.885360

Mn^{II} Complexes with a Novel Triacid as Ligand: Synthesis and Characterization

DEHAI ZHAO,[1] ZHENJUN SI,[1,*] TAO SHI,[1] QIAN DUAN,[1] AND LINFANG SHI[2]

[1]School of Materials Science and Engineering, Changchun University of Science and Technology, Hangchun, P. R. China
[2]College of Sciences, Zhejiang A & F University, Lin'an, P. R. China

*A novel aromatic tricarboxylic acid of 4,4′-(2-carboxypropane-1,3-diyl)dibenzoic acid (H_3L) was used to prepare two Mn^{II} complexes of $[Mn_3(L)_2(bpy)_2]_n$ (**1**) and $[Mn_3(L)_2(phen)_2]_n$ (**2**), where bpy = 2,2′-bipyridine and phen = 1,10-phenanthroline. The single crystal structures, thermal stability, and the magnetism of **1** and **2** were measured and discussed in this article. According to the magnetism measurements, the Curie constants and the Weiss constants should be 12.29 $K{\cdot}cm^3{\cdot}mol^{-1}$ ($g = 1.94$, $S = 5/2$) and -9.80 K for **1** and 11.11 $K{\cdot}cm^3{\cdot}mol^{-1}$ ($g = 1.83$, $S = 5/2$) and -9.26 K for **2**, respectively.*

Keywords Magnetism; Mn^{II} complexes; X-ray diffraction

Introduction

In the past decades, the synthesis and studies on the metal complexes [1–10], especially those with multiunclears [1,3,5], have increased greatly due to the potential that such compounds display for new technological applications. In order to explore the applications of the metal complexes, it is critical to design and synthesis novel organic compounds that can be used as the ligands in metal complexes [11–17]. As an important kind of ligand, the organic acids [15–17], especially the nonconjugated aromatic acids, were extensively applied to construct the metal complexes because the carboxyl groups of organic acids can act as not only the coordination groups but also the donor and/or acceptors of the hydrogen bonds [18,19]. Furthermore, the alkyl linkers of the nonconjugated aromatic polycarboxylic acids can change their spatial structures to meet the coordination requirements of the metal complexes [20–24], and the aromatic rings can give the aromatic polycarboxylic acids some additional molecular forces such as π–π stacking and π–H interactions [25,26]. For example, Wang et al. and Chen et al. reported that the nonconjugated aromatic polycarboxylic acids with an atom between the aromatic rings are useful to prepare metal complexes with unexpected structures and/or excellent properties [21,22], and our group recently

*Address correspondence to Zhenjun Si and Qian Duan, School of Materials Science and Engineering, Changchun University of Science and Technology, Hangchun 130022, P. R. China.; Fax: +86 431 85583015; E-mail: szj@cust.edu.cn, duanqian88@hotmail.com

Color versions of one or more of the figures in the article can be found online at www.tandfonline.com/gmcl.

synthesized two Co^{II} complexes using a dicarboxylic acid of 4,4′-(2-acetylpropane-1,3-diyl)dibenzoic acid as ligand [23].According to the above mentioned researches, we use a tricarboxylic acids of 4,4'-(2-carboxypropane-1,3-diyl)dibenzoic acid (H_3L), which have 1,3-propylidene group between the aromatic rings as the organic ligand, to hydrothermally synthesize two Mn^{II} complexes of $[Mn_3L_2(bpy)_2]_n$ (**1**) and $[Mn_3L_2(phen)_2]_n$ (**2**) (where bpy = 2,2′-bipyridine and phen = 1,10-phenanthroline). And the X-ray single crystal diffraction, the infrared (IR) spectroscopy, thermogravimetric analyses (TGA) and magnetic analyses were applied to characterize **1** and **2**.

Experimental Section

Materials and Instrumentation

All chemicals and reagents from the commercial sources were used without further purification. H_3L was synthesized according to the previously reported methods [27,28]. IR spectra were recorded on a FTIR-8400S SHIMADZU spectrophotometer in the 4000–400 cm^{-1} region with KBr pellets. The crystal structures of **1** and **2** were measured on a Bruker Smart Apex CCD single-crystal diffractometer using Mo Kα radiation, $\lambda = 0.7107$ Å at 293 K. The powder X-ray diffraction (XRD) patterns were recorded on a Ultima IV X-ray diffractometer. The TGA was performed on **1** and **2** using a Perkin-Elmer thermal analyzer. The molecular structures were solved using the SHELXL-97 program, [29–31]. The magnetic susceptibility data were collected in the magnetic field of 1000 Oe on a MPMS RSO with the temperature range of 2–300 K.

Synthesis of $[Mn_3(L)_2(bpy)_2]_n$ (1)

A mixture of $Mn(CH_3COO)_2{\cdot}4H_2O$ (24.5 mg, 0.1 mmol), H_3L (32.8 mg, 0.1 mmol), and bpy (15.6 mg, 0.1 mmol) was stirred in water (3.0 mL) and the pH of the mixture was adjusted to 6.5 with ammonia aqueous solution, and then sealed in a 5-mL Telfon-lined stainless-steel container, which was heated to 170°C for 72 hr and then cooled to room temperature at a rate of $5°C{\cdot}hr^{-1}$. Yellow block crystals were collected as a single phase, judging by the powder XRD measurement. Yield: ca. 56.0%. IR (KBr): 3560, 1604, 1411, 1089, 1023, 876, cm^{-1}.

Synthesis of $[Mn_3(L)_2(phen)_2]_n$ (2)

Compound **2** were synthesized in the same way to **1** by replacing bpy with phen. The yellow block crystals of **2** were collected as a single phase, judging by the powder XRD measurement. Yield: ca. 57.1%. IR (KBr): 3450, 1598, 1423, 1135, 1021, 898 cm^{-1}.

Results and Discussion

Crystal Structures

The crystal data of **1** and **2** are listed in Table 1, and the selective bond distances and the bond angles of **1** and **2** are listed in Tables 2 and 3, respectively. According to the ORTEP view of **1** in Fig. 1(A), Mn(1) is coordinated by four aromatic carboxyl oxygen atoms (O(4), O(4)#1, O(6), and O(6)#1) and two aliphatic carboxyl oxygen atoms (O(2) and O(2)#1), which are from six different L^{3-} ligands, while Mn(2) is coordinated by three aromatic carboxyl oxygen atoms (O(3), O(5), and O(6)) and an aliphatic carboxyl oxygen atom (O(1)) of three

Table 1. Crystal data of **1** and **2**

	1	2
Formula	$[Mn_3(L)_2(bpy)_2]_n$	$[Mn_3(L)_2(phen)_2]_n$
FW	1127.76	1175.80
Cryst. Syst.	triclinic	monoclinic
Space group	P-1	P 21/c
A (Å)	9.333(3)	12.1356(7)
B (Å)	12.059(3)	21.1552(12)
C (Å)	12.461(4)	10.1989(6)
α (deg)	61.478(4)	90
β (deg)	87.962	106.2400(10)
γ (deg)	77.131	90
V ($Å^3$)	1197.1(6)	2513.9(3)
Z	1	2
$\rho_{calc.}$ (Mg/m^3)	1.564	1.553
μ (mm^{-1})	0.852	0.815
F(000) (e)	577	1202.0
θ for collection (deg)	1.87–25.08	1.75–26.12
Completeness	97.3%	99.7%
Reflections collected	5917	13831
Goodness-of-fit on F^2	0.958	1.041
R1, wR2 [$I > 2\sigma(I)$]	0.0661, 0.1386	0.0446, 0.0907
R1, wR2 (all data)	0.1412, 0.1720	0.0782, 0.1040

Table 2. Selective bond distances (Å) and bond angles (°) of **1**

Mn(1)–O(6)	2.124(4)	Mn(2)–O(1)	2.038(4)
Mn(1)–O(6)#1	2.124(4)	Mn(2)–O(3)	2.080(4)
Mn(1)–O(2)#1	2.190(5)	Mn(2)–O(5)	2.226(4)
Mn(1)–O(2)	2.190(5)	Mn(2)–O(6)	2.456(4)
Mn(1)–O(4)#1	2.291(4)	Mn(2)–N(1)	2.228(5)
Mn(1)–O(4)	2.291(4)	Mn(2)–N(2)	2.336(5)
O(6)–Mn(1)–O(6)#1	180.000(1)	O(1)–Mn(2)–O(3)	152.3(2)
O(6)–Mn(1)–O(2)#1	94.70(17)	O(1)–Mn(2)–O(5)	92.85(18)
O(6)#1–Mn(1)–O(2)#1	85.30(17)	O(3)–Mn(2)–O(5)	99.63(18)
O(6)–Mn(1)–O(2)	85.30(17)	O(1)–Mn(2)–N(1)	109.6(2)
O(6)#1–Mn(1)–O(2)	94.70(17)	O(3)–Mn(2)–N(1)	94.43(19)
O(2)#1–Mn(1)–O(2)	180.000(1)	O(5)–Mn(2)–N(1)	93.19(17)
O(6)–Mn(1)–O(4)#1	91.32(15)	O(1)–Mn(2)–N(2)	83.02(18)
O(6)#1–Mn(1)–O(4)#1	88.68(15)	O(3)–Mn(2)–N(2)	91.89(19)
O(2)#1–Mn(1)–O(4)#1	94.78(16)	O(5)–Mn(2)–N(2)	161.8(2)
O(2)–Mn(1)–O(4)#1	85.22(16)	N(1)–Mn(2)–N(2)	71.80(19)
O(6)–Mn(1)–O(4)	88.68(15)	O(1)–Mn(2)–O(6)	82.39(16)
O(6)#1–Mn(1)–O(4)	91.32(15)	O(3)–Mn(2)–O(6)	84.27(16)
O(2)#1–Mn(1)–O(4)	85.22(16)	O(5)–Mn(2)–O(6)	56.01(15)
O(2)–Mn(1)–O(4)	94.78(16)	N(1)–Mn(2)–O(6)	148.16(16)
O(4)#1–Mn(1)–O(4)	180.000(1)	N(2)–Mn(2)–O(6)	139.97(18)

Symmetry codes: #1, $-x+2$, $-y+1$, $-z+2$; #2, x, y, $z-1$; #3, x, y, $z+1$; #4, $x+1$, y, z; #5, $x-1$, y, z.

Table 3. Selective bond distances (Å) and bond angles (°) of **2**

Mn(1)–O(1)	2.1229(19)	Mn(2)–O(2)	2.085(2)
Mn(1)–O(1)#5	2.1229(19)	Mn(2)–O(4)	2.105(2)
Mn(1)–O(3)	2.264(2)	Mn(2)–O(5))	2.349(2)
Mn(1)–O(3)#5	2.264(2)	Mn(2)–O(6)	2.286(2)
Mn(1)–O(5)	2.111(2)	Mn(2)–N(1)	2.289(3)
Mn(1)–O(5)#5	2.111(2)	Mn(2)–N(2)	2.336(2)
O(5)#5–Mn(1)–O(5)	180.00(11)	O(2)–Mn(2)–O(4)	134.49(9)
O(5)#5–Mn(1)–O(1)#5	90.01(8)	O(2)–Mn(2)–O(6)	107.11(9)
O(5)–Mn(1)–O(1)#5	90.00(8)	O(4)–Mn(2)–O(6)	102.16(9)
O(5)#5–Mn(1)–O(1)	90.00(8)	O(2)–Mn(2)–N(1)	100.09(9)
O(5)–Mn(1)–O(1)	90.00(8)	O(4)–Mn(2)–N(1)	119.10(10)
O(1)#5–Mn(1)–O(1)	180.00(12)	O(6)–Mn(2)–N(1)	79.64(8)
O(5)#5–Mn(1)–O(3)	99.96(9)	O(2)–Mn(2)–N(2)	79.10(9)
O(5)–Mn(1)–O(3)	80.04(9)	O(4)–Mn(2)–N(2)	91.65(9)
O(1)#5–Mn(1)–O(3)	91.83(8)	O(6)–Mn(2)–N(2)	151.04(8)
O(1)–Mn(1)–O(3)	88.17(8)	N(1)–Mn(2)–N(2)	71.40(9)
O(5)#5–Mn(1)–O(3)#5	80.04(9)	O(2)–Mn(2)–O(5)	81.84(8)
O(5)–Mn(1)–O(3)#5	99.96(9)	O(4)–Mn(2)–O(5)	87.43(9)
O(1)#5–Mn(1)–O(3)#5	88.17(8)	O(6)–Mn(2)–O(5)	55.06(8)
O(1)–Mn(1)–O(3)#5	91.83(8)	N(1)–Mn(2)–O(5)	132.27(8)
O(3)–Mn(1)–O(3)#5	180.00(9)	N(2)–Mn(2)–O(5)	152.23(8)

Symmetry codes: #1, $-x+1$, $y-1/2$, $-z+1/2$; #2, $-x+1$, $y+1/2$, $-z+1/2$; #3, x, y, $z+1$; #4, x, y, $z-1$; #5, $-x+1$, $-y$, $-z$.

different L^{3-} ligands and two nitrogen atoms (N(1) and N(2)) from a phen molecule. The bond distances of Mn(1)–O(2) (2.190(5) Å), Mn(1)–O(4) (2.291(4) Å), and Mn(1)–O(6) (2.124(4) Å) are equals to those of Mn(1)–O(2)#1, Mn(1)–O(4)#1, and Mn(1)–O(6)#1, respectively. The bond distances of Mn(2)–O are in the range of 2.038(4)–2.456(4) Å, and the bond distances of Mn(2)–N(1) and Mn(2)–N(2) are 2.228(5) and 2.336(5) Å, respectively. The bond angles of O(6)–Mn(1)–O(6)#1, O(2)–Mn(1)–O(2)#1, and O(4)–Mn(1)–O(4)#1 are equal to each other with the value of 180.000(1)°. The bond angles of O(1)–Mn(2)–O(3), N(1)–Mn(2)–N(2), O(5)–Mn(2)–O(6), N(1)–Mn(2)–O(6), O(5)–Mn(2)–N(2), and N(2)–Mn(2)–O(6) are 152.3(2), 71.80(19), 56.01(15), 148.16(16), 161.8(2), and 139.97(18)°, respectively, to adapt for the coordination requirement of Mn(2). The other bond angles with the Mn^{II} ion as the apex are around 90°. Mn(1) and two symmetrical Mn(2) ions form the tri-nuclear centers with the distance of 7.107 Å between Mn(2) and Mn(2)' which parallel to each other. It is found that each unit cell of crystal **1**, containing four tri-nuclear centers, presents a hole with the radius of 3 Å (B), which is further connected by the deprotonated L^{3-} ligands to form the 2D network structure (Fig. 1(C)).

The coordination environment of Mn^{II} and the L^{3-} in crystal **2** are presented in Fig. 2(A) and (B), respectively. As can be seen in Fig. 2(A), Mn(1) is coordinated by four aromatic carboxylic oxygen atoms (O(1), O(1)#5, O(3),O(3)#5) and two aliphatic carboxyl oxygen atoms (O(5) and O(5)#5) in six different L^{3-} ligands, Mn(2) is coordinated by two aromatic carboxylic oxygen atoms (O(2) and O(4)) and an aliphatic carboxyl group (O(5) and O(6)) in three different L^{3-} ligands. The bond distances of Mn(1)–O(1), Mn(1)–O(3), and Mn(1)–O(5) are equal to those of Mn(1)–O(1)#5, Mn(1)–O(3)#5,

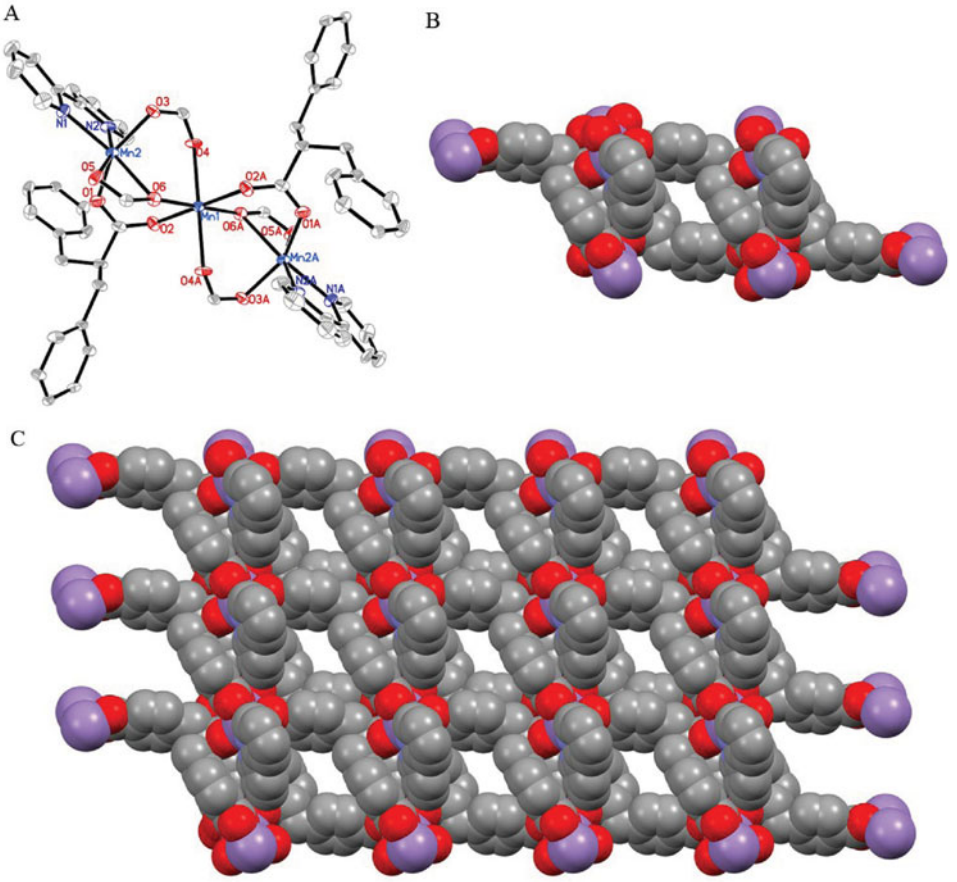

Figure 1. ORTEP drawing with 30% thermal ellipsoids (A), unit cell structure (B), and 2D network structure (C) viewed in b* direction of **1**, hydrogen atoms are omitted for the clarity.

and Mn(1)–O(5)#5 with the values of 2.1229(19), 2.264(2), and 2.111(2) Å, respectively, while the bond distances of Mn(2)–O(2), Mn(2)–O(4), Mn(2)–O(5), Mn(2)–O(6), Mn(2)–N(1), and Mn(2)–N(2) are 2.085(2), 2.105(2), 2.349(2), 2.286(2), 2.289(3), and 2.336(2) Å, respectively. The bond angles of O(5) –Mn(1)–O(5)#5, O(1)–Mn(1)–O(1)#5 and O(3)–Mn(1)–O(3)#5 are equal to each other with the value of 180.00°. The bond agnles of O(6)–Mn(2)–O(5), N(1)–Mn(2)–N(2), O(2)–Mn(2)–O(4), O(6)–Mn(2)–N(2), N(1)–Mn(2)–O(5), and N(2)–Mn(2)–O(5) are 55.06(8), 71.40(9), 134.49(9), 151.04(8), 132.27(8), and 152.23(8)°, respectively, to adapt for the coordination requirement of Mn(2). The other bond angles with Mn^{II} ion as the apex are around 90°. Similar to **1**, the tri-nuclear centers in **2**, which contain a Mn(1) ion and two symmetrical Mn(2) ions with the distance of 7.425 Å between Mn(2) and Mn(2)′, are also linked by L^{3-} ligands to form the 2D coordination polymers (Fig. 2(C)). But with the replace of the bpy of **1** with phen, these tri-nuclear centers of **2** are alternately arranged in two directions with the angle of 56.056 (17)°, which leads to the absence of the holes in the 2D structure of **2**.

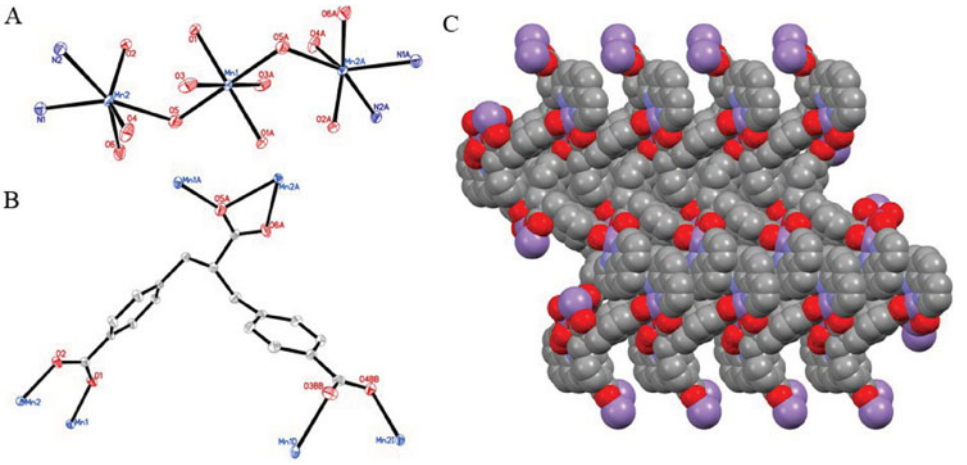

Figure 2. ORTEP drawing of coordination environment of Mn^{II} (A) and L^{3-} ion (B) with 30% thermal ellipsoids and 2D network structure (C) viewed in a* direction of **2** (C), hydrogen atoms are omitted for the clarity.

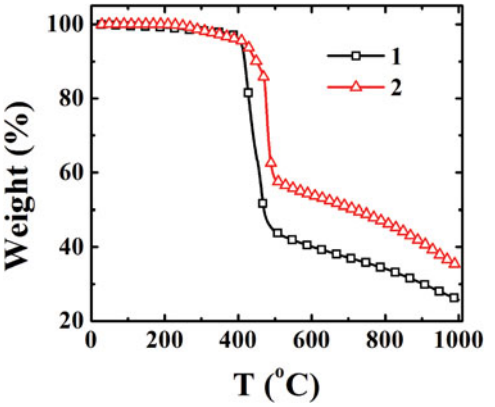

Figure 3. TGA diagrams of **1** and **2**.

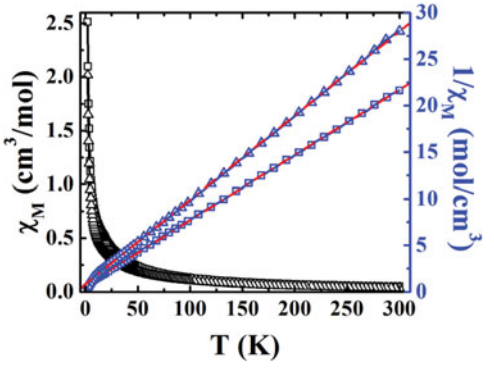

Figure 4. Magnetic properties of **1** (square) and **2** (triangle) in the form of χ_M versus T (black) and $1/\chi_M$ versus T (blue).The red dash-dot lines are the fitting results.

Thermal Stability

TGA of **1** and **2** were carried out under N_2 atmosphere in the range of 50°C—1000°C to study their thermal stability, the corresponding curves are presented in Fig. 3. It is found that the weight loss of **1** and **2** should be ca. 4% and ca. 6%, respectively, when they were heated up to 400°C under N_2 atmosphere. With the further increase of the temperature, **1** and **2** begin to dramatically decompose at ca. 405 and 417°C, respectively, and remains ca. 44.0% and ca. 58.0%, respectively, when they were heated up to 500°C. These data suggest that both **1** and **2** possess the excellent thermal stability.

Magnetism

The plots of the χ_m and $1/\chi_m$ versus temperature (T) of **1** and **2** are depicted in Fig. 4. The $\chi_m T$ of **1** and **2** were measured at 300 K to be 13.88 $K{\cdot}cm^3/mol$ and 14.12 $K{\cdot}cm^3/mol$, respectively, which nicely accord with the expected $\chi_m T$ of 13.725 $cm^3{\cdot}K{\cdot}mol^{-1}$ for three isolate Mn^{2+} ions ($g = 2.00$ and $S = 5/2$). Fitting the data of the χ_m versus T of **1** and **2** to the Curie–Weiss law, $\chi_m = C/(T - \theta)$, the values of the Curie constants (C) and the Weiss constants (θ) are simulated to be 12.29 $K{\cdot}cm^3{\cdot}mol^{-1}$ ($g = 1.94$, $S = 5/2$) and -9.80 K for **1** and 11.11 $K{\cdot}cm^3{\cdot}mol^{-1}$ ($g = 1.83$, $S = 5/2$) and -9.26 K for **2**, respectively. These results suggest that the bigger molecular structure of the phen in crystal **2** leads to the lower value of C. The negative Weiss constants indicate the antiferromagnetic coupling dominating the crystals of **1** and **2** [32,33]. Therefore, the typical paramagnetic behaviors of **1** and **2** should be ascribed to the incomplete cancellation of antiferromagnetic coupling between the magnetic centers.

Conclusions

In summary, the aromatic tricarboxylic acids (H_3L) was applied to prepare two Mn^{II} complexes **1** and **2** whose single crystal structures, thermal stability and the magnetic properties characterized and studied. Fitting the data to the Curie-Weiss law, the θ was calculated to be -9.80 K ($g = 1.94$, $S = 5/2$) for **1** and -9.26 K ($g = 1.83$, $S = 5/2$) for **2**, respectively. These negative values of θ indicate there should be antiferromagnetic coupling in **1** and **2**. Additionally, this study revealed that the bigger molecular structure of the phen in crystal **2** leads to not only the bigger value of the distance between the Mn^{II} ions in the tri-nuclear centers but also the lower value of C, which should be helpful for the further design of the magnetic metal complexes.

Supporting Information (see footnote on the first page of this article): Crystallographic data for the structural analysis have been deposited with the Cambridge Crystallographic Data Center, CCDC reference number: 936309 for **1** and 936310 for **2**. This data can be obtained free of charge from the Cambridge Crystallographic Data Centre via www.ccdc.cam.ac.uk/data_request/cif.

Acknowledgment

The authors are grateful to financial aid from the National Natural Science Foundation of China (Grant No. 21271033) and Natural Science Foundation of Zhejiang Province (Grant No. LY12B02013).

References

[1] Suh, M. P., Park, H. J., Prasad, T. K., & Lim, D. W. (2012). *Chem. Rev.*, *112*, 782.
[2] Rowsell, J. L. C., & Yaghi, O. M. (2005). *Angew. Chem. Int. Ed.*, *44*, 4670.
[3] Nouar, F., Eubank, J. F., Bousquet, T., Wojtas, L., Zaworotko, M. J., & Eddaoudi, M. (2008). *J. Am. Chem. Soc.*, *130*, 1833.
[4] Forgan, R. S., Sauvage, J. P., & Stoddart, J. F. (2011). *Chem. Rev.*, *111*, 5434.
[5] Liu, S.-J., Xue, L., Hu, T.-L., & Bu, X.-H. (2012). *Dalton Trans.*, *41*, 6813.
[6] Wang, X. Y., Wang, L., Wang, Z. M., Su, G., & Gao, S. (2005). *Chem. Mater.*, *17*, 6369.
[7] Chakrabarty, R., Mukherjee, P. S., & Stang, P. J. (2011). *Chem. Rev.*, *111*, 6810.
[8] Lin, X. A., Black, J., Wilson, C., Sun, X. Z., Champness, N. R., George, M. W., Hubberstey, P., Mokaya, R., & Schröder, M. (2006). *J. Am. Chem. Soc.*, *128*, 10745.
[9] Zhao, X., Xiao, B., Fletcher, A. J., Thomas, K. M., Bradshaw, D., & Rosseinsky, M. J. (2004). *Science*, *306*, 1012.
[10] Chu, Q., Su, Z., Fan, J., Okamura, T., Lv, G. C., Liu, G. X., Sun, W. Y., & Ueyama, N. (2011). *Cryst. Growth Des.*, *11*, 3885.
[11] Tong, G. S. M., Law, Y. C., Kui, S. C. F., Zhu, N., Leung, K. H., Phillips, D. L., & Che, C. M. (2010). *Chem. Eur. J.*, *16*, 6540.
[12] Tong, J., Yu, S. Y., & Li, H. (2012). *Chem. Commun.*, *48*, 5343.
[13] Kim, J. I., Kwak, H. Y., Yoon, J. H., Ryu, D. W., Yoo, I. Y., Yang, N., Cho, B. K., Park, J. G., Lee, H., & Hong, C. S. (2009). *Inorg. Chem.*, *48*, 2956.
[14] Gillett-Kunnath, M. M., Paik, J. I., Jensen, S. M., Taylor, J. D., & Sevov, S. C. (2011). *Inorg. Chem.*, *50*, 11695.
[15] García-Zarracino, R., & Höpfl, H. (2004). *Angew. Chem. Int. Ed.*, *43*, 1507.
[16] García-Zarracino, R., & Höpfl, H. (2005). *J. Am. Chem. Soc.*, *127*, 3120.
[17] Kitagawa, S., Kitaura, R., & Noro, S. (2004). *Angew. Chem. Int. Ed.*, *43*, 2334.
[18] Li, H., Eddaoudi, M., O'Keeffe, M., & Yaghi, O. M. (1999). *Nature*, *402*, 276.
[19] De Lill, D. T., Gunning, N. S., & Cahill, C. L. (2005). *Inorg. Chem.*, *44*, 258.
[20] Lan, Y. Q., Li, S. L., Shao, K. Z., Wang, X. L., Du, D. Y., Su, Z. M., & Wang, D. J. (2008). *Cryst. Growth Des.*, *8*, 3490.
[21] Liu, J. Q., Wang, Y. Y., Zhang, Y. N., Liu, P., Shi, Q. Z., & Batten, S. R. (2009). *Eur. J. Inorg. Chem.*, 147.
[22] Chen, X. L., Guo, L., Hu, H. M., Fu, F., Han, Z. X., Shu, H. M., Yang, M. L., Xue, G. L., & Du, C. Q. (2008). *Eur. J. Inorg. Chem.*, *2008*, 239.
[23] Guo, Y., Shi, T., Si, Z., Duan, Q., & Shi, L. (2013). *Inorg. Chem. Comm.*, *34*, 15.
[24] Xiao, D. R., Wang, E. B., An, H. Y., Li, Y. G., Su, Z. M., & Sun, C. Y. (2006). *Chem. Eur. J.*, *12*, 6528.
[25] Zhou, Z. H., Yang, J. M., & Wan, H. L. (2005). *Cryst. Growth Des.*, *5*, 1825.
[26] Wei, Y. Q., Yu, Y. F., Sa, R. J., Li, Q. H., & Wu, K. C. (2009). *Cryst. Eng. Comm.*, *11*, 1054.
[27] Johnson, A. W., Markham, E., & Price, R. (1973). *Org. Synth.*, *5*, 785.
[28] Boatman, S., & Hauser, C. R. (1973). *Org. Synth.*, *5*, 767.
[29] Sheldrick, G. M. (1998). *SHELXTL*, version 5.10, Siemens Analytical X-ray Instruments Inc.: Madison, WI.
[30] SMART and SAINT (1995). Siemens Analytical X-ray Instruments Inc.: Madison, WI.
[31] Sheldrick, G. M. (1996). *SADABS*, University of Göttingen: Göttingen, Germany.
[32] Carlin, R. L. (1981). *Magnetochemistry*, Springer-Verlag: New York.
[33] Kahn. (1993). *Molecular Magnetism*, VCH: New York.